Development of New Exchange-Correlation Functionals. 2

David J. Tozer* and Nicholas C. Handy

Department of Chemistry, University of Cambridge, Cambridge, CB2 1EW, U.K.

Received: November 19, 1997; In Final Form: February 18, 1998

We recently presented a new method for developing exchange-correlation functionals using ab initio numerical exchange-correlation potentials and accurate total energies. A preliminary functional was presented. In this paper we refine the functional expansion and demonstrate that significantly improved atomization energies can be obtained by amending the fitting procedure to include atomization energies rather than total molecular energies. A new functional is presented that provides an improved description of simple first-row hydrogen abstraction reactions compared to conventional continuum density functionals. This improvement is achieved without introducing any fraction of exact orbital exchange.

1. Introduction

In our first paper on this topic,[1] hereafter denoted paper I, we presented a method for developing new generalized gradient approximation (GGA) exchange-correlation functionals from ab initio and energetic data. Several aspects of the new functionals differ significantly from those of conventional functionals.

(i) The functionals represent exchange and correlation effects in a combined manner. Individual exchange and correlation terms cannot be isolated, which is consistent with the view that the two are not trivially separable. For example, the failure of restricted Hartree−Fock (RHF) theory to provide an accurate description of dissociation is usually attributed to the lack of correlation in the method. However, the RHF energy of infinitely separated H_2 is in error by an exchange integral. Second, it is often stated, though not fully understood, that exchange functionals must include nondynamic correlation effects.

(ii) The new functionals do not include any exact orbital exchange. Although adiabatic arguments indicate that it should enter, we do not feel it is an essential feature of a quality functional. The optimized effective potential (OEP)[2] successfully represents atomic Hartree−Fock properties, suggesting that a GGA functional should be able to represent adequately the effect of exact exchange. Like the OEP, an exchange GGA potential is multiplicative and so, for an asymptotically vanishing exchange-correlation potential, the ith Kohn−Sham orbital asymptotically behaves as $\exp(-(-2\epsilon_i)^{1/2}r)$. In contrast, the presence of conventional nonmultiplicative exchange constrains the asymptotic behavior of all the orbitals to be governed by the HOMO eigenvalue,[3] which is less desirable from a physical viewpoint. Finally, although exchange-correlation potentials appear to be reasonably well-behaved, correlation potentials in the Hartree−Fock−Kohn−Sham formalism are highly oscillatory.[4] The inclusion of exact exchange can therefore lead to a residual which is difficult to represent by a density functional.

(iii) Conventional functionals are often based on the local density approximation[5] (LDA). This is derived from a free-electron gas, which is a poor representation of a molecular system, and it follows that LDA predicts poor asymptotic densities. Gradient corrections are added to the LDA with the aim of improving the energetics, although since the asymptotic density contributes little to the energetics, this procedure does not remove the underlying error in the asymptotic regions. In contrast, our new functionals are not based on the LDA but are instead determined by a fitting procedure involving both energetics and exchange-correlation potentials. The inclusion of the potential provides information from the entire molecular environment and should result in improved asymptotic densities. Furthermore, if our functionals can reproduce accurate exchange-correlation potentials, then accurate optimized geometries must follow, since the error in geometries from conventional continuum functionals arises, for a given basis set, due to the error in the exchange-correlation potential. (Of course, we recognize that fitting to potentials is not the only way to develop functionals that yield accurate structural predictions; such functionals may also be determined by introducing exact orbital exchange, and fitting to energetic data alone.)

(iv) Our investigations[1,6] highlighted the requirement that for a continuum functional to achieve both accurate energetics and asymptotic densities, its exchange-correlation potential must not vanish asymptotically. This feature, which is a consequence of integer derivative discontinuities in the energy, had already been demonstrated theoretically in 1982 by Perdew, Parr, Levy, and Balduz[7] (PPLB) but had not been previously observed in practical implementations due to the tendency to develop functionals with accurate energetics but not accurate asymptotic densities.

It can be shown that in a restricted formalism, the asymptotic potential should be the hardness $(I - A)/2$ (where I and A are the ionization energy and electron affinity, respectively) for degenerate open-shell systems,[8] and less than the hardness for closed-shell systems. The exchange-correlation potential is therefore the asymptotically vanishing potential, which gives the exact density, shifted at all points by the value of the asymptotic potential. Consequently, for open-shell systems, the HOMO eigenvalue is not $-I$, which would be the eigenvalue if the potential vanished asymptotically, but $-(I + A)/2$, the negative of the electronegativity. It is well-known that conventional functionals do give eigenvalues close to this quantity, and so rather than indicating a failure of conventional functionals, this indicates that conventional exchange-correlation potentials resemble the shifted PPLB potentials in energetically important regions. This feature is crucial if a continuum functional is to give accurate energetics: a functional that yields an accurate density with a vanishing asymptotic potential gives a severely underestimated exchange-correlation energy because the potential in energetically important regions lies well below that of PPLB and conventional functionals.[6]

S1089-5639(98)00259-X CCC: $15.00
Published on Web 04/11/1998

In asymptotic regions, the potentials of conventional continuum density functionals such as BLYP[9] approach zero, and so no longer resemble those of PPLB. Although these regions contribute little to the energy, this discrepancy means the asymptotic density behaves as

$$\lim_{r\to\infty}\rho(\mathbf{r}) \sim \exp(-2(-2\epsilon_N)^{1/2}r) \tag{1}$$

where N denotes the HOMO orbital, and so for an open-shell system

$$\lim_{r\to\infty}\rho(\mathbf{r}) \sim \exp(-2(I+A)^{1/2}r) \tag{2}$$

where A is typically much less than I. The asymptotic density from conventional functionals is therefore much more diffuse than the exact density[10]

$$\lim_{r\to\infty}\rho^0(\mathbf{r}) \sim \exp(-2(2I)^{1/2}r) \tag{3}$$

and this is consistent with observed overestimated polarizabilities and bond lengths. To improve conventional functionals, it is therefore necessary to slow the decay of the asymptotic potential—while leaving the potential in energetically important regions (and thus the energetics) relatively unchanged—such that it approaches the nonzero positive value of PPLB. By approaching this nonzero value k, the density behaves as

$$\lim_{r\to\infty}\rho(\mathbf{r}) = \exp(-2(-2[\epsilon_N - k])^{1/2}r) \tag{4}$$

For open-shell systems where k is the hardness and ϵ_N is the negative of the electronegativity, the exact asymptotic density clearly follows

$$\lim_{r\to\infty}\rho(\mathbf{r}) \sim \exp\left(-2\left(-2\left[-\frac{(I+A)}{2}-\frac{(I-A)}{2}\right]\right)^{1/2}r\right) \sim \exp(-2(2I)^{1/2}r) \tag{5}$$

It is nontrivial to amend conventional functionals such that only their asymptotic potentials change. However, by including the potential in our fit, our approach offers a convenient way to achieve potentials resembling those of PPLB. Functionals are obtained whose potentials closely resemble conventional potentials in energetically important regions but approach nonzero values asymptotically. The method is summarized in section 2, with particular emphasis on recent improvements that have been made. In section 3 we present a new functional and examine its energetics for a set of small first-row molecules. In section 4 we investigate six simple hydrogen abstraction reactions. Conclusions are presented in section 5.

2. Methodology

The new exchange-correlation functional is defined as

$$E_{\text{fit}} = \int F_{\text{xc}}(\rho_\alpha,\rho_\beta,\zeta_\alpha,\zeta_\beta,\zeta_{\alpha\beta})\,\mathrm{d}\mathbf{r} \tag{6}$$

where

$$\zeta_\alpha = |\nabla\rho_\alpha| \tag{7}$$

$$\zeta_\beta = |\nabla\rho_\beta| \tag{8}$$

$$\zeta_{\alpha\beta} = \nabla\rho_\alpha\cdot\nabla\rho_\beta \tag{9}$$

with

$$F_{\text{xc}} = \sum_{abcd}\omega_{abcd}R^aS^bX^cY^d = \sum_{abcd}\omega_{abcd}f_{abcd}(\mathbf{r}) \tag{10}$$

where ω_{abcd} are variable parameters and

$$R^a \equiv \rho_\alpha^a + \rho_\beta^a \tag{11}$$

$$S^b \equiv \left(\frac{\rho_\alpha-\rho_\beta}{\rho}\right)^{2b} \tag{12}$$

$$X^c \equiv \frac{\zeta_\alpha^c+\zeta_\beta^c}{2\rho^{4c/3}} \tag{13}$$

$$Y^d \equiv \left(\frac{\zeta_\alpha^2+\zeta_\beta^2-2\zeta_{\alpha\beta}}{\rho^{8/3}}\right)^d \tag{14}$$

$$\rho = \rho_\alpha + \rho_\beta \tag{15}$$

To compute optimal parameters, a training set of systems is chosen. In this paper we use the same first-row training set as that of paper I, namely, the ground states of H, Li, C, N, O, F, NH_2, CH, CH_2, O_2, Ne, CH_4, CO, F_2, BH, H_2, H_2O, N_2, LiH, and HF. For each training system, correlated ab initio electron densities are computed. For closed-shell systems the coupled cluster BD method[11] is used, while unrestricted second-order Møller−Plesset theory is used for the open-shell systems. TZ2P basis sets are used throughout.[12,13] These densities are then fed into a basis set implementation of the Zhao, Morrison, Parr (ZMP)[14] procedure and asymptotically vanishing exchange-correlation potentials—denoted ZMP potentials—are computed on numerical quadrature grids. A functional whose potential resembles the ZMP potential gives a very poor exchange-correlation energy because the potential vanishes asymptotically. Following PPLB and paper I, we require a functional whose potential resembles the ZMP potential shifted by some appropriate system-dependent value. In an unrestricted framework, this is achieved by minimizing the term

$$\Omega_V = \sum_M\sum_\sigma^{\alpha,\beta}\int \mathrm{d}\mathbf{r}\,[v_{\text{zmp}}^{M\sigma}(\mathbf{r}) + k_{M\sigma} - v_{\text{fit}}^{M\sigma}(\mathbf{r})]^2\rho_{M\sigma}^q(\mathbf{r}) \tag{16}$$

where $v_{\text{zmp}}^{M\sigma}(\boldsymbol{r})$ is the σ ZMP potential for training system M, $k_{M\sigma}$ represents the unknown shift between the ZMP and exact continuum σ potential for system M, $v_{\text{fit}}^{M\sigma}(\boldsymbol{r})$ is the σ potential of the fitted functional for system M, and $\rho_{M\sigma}^q(\boldsymbol{r})$ is a weighting factor. The value of $k_{M\sigma}$ influences the exchange-correlation energy of the functional, and its value must be computed self-consistently. To do this, we must define a term that, when minimized, ensures that the energetics are accurately described. In paper I, where the functional denoted TH1 was developed, this contribution was the sum of the squares of the errors in the exchange-correlation energy of the fitted functional

$$\Omega_E^{TH1} = \sum_M w_M[E_{\text{xc}}^M - E_{\text{fit}}^M]^2 \tag{17}$$

The exact energies E_{xc}^M are not known and so are approximated as

$$E_{\text{xc}}^M = E_{\text{tot},0}^M - T_s[\rho_M] - J[\rho_M] - E_{\text{ne}}[\rho_M] - E_{\text{nuc}} \tag{18}$$

where ρ_M is the ab initio density of system M, $T_s[\rho_M]$ is the noninteracting kinetic energy associated with the Kohn−Sham orbitals from the ZMP procedure, and $E_{tot,0}^M$ is the near-exact

total molecular energy computed from atomic energies and experimental atomization and zero-point energies.[15] In the next section we demonstrate that although this definition of Ω_E leads to accurate total energies, it gives less accurate atomization energies. In this paper, we therefore choose to redefine Ω_E as

$$\Omega_E = \sum_{M=\text{atoms}} w_M[E^M_{\text{xc}} - E^M_{\text{fit}}]^2 + \sum_{M=\text{mols}} w_M[AE^M_{\text{xc}} - AE^M_{\text{fit}}]^2 \tag{19}$$

where the first contribution measures the error in the exchange-correlation energies of the atoms in the training set, while the second term measures the error in the exchange-correlation contribution AE^M_{xc} to the atomization energies of the molecules in the training set. Approximations to AE^M_{xc} are trivially obtained from E^M_{xc}.

The optimum parameters and shifts are then computed by minimizing the quantity

$$\Omega = \Omega_V + \Omega_E \tag{20}$$

with respect to ω_{abcd} and $k_{M\sigma}$. (In paper I, a slightly different approach was used to compute the shifts.) In practical terms, we choose initial values for $k_{M\sigma}$ and determine ω_{abcd} from

$$\left.\frac{\partial\Omega}{\partial\omega_{abcd}}\right|_{k_{M\sigma}} = 0 \tag{21}$$

Using this solution, we then compute improved values for $k_{M\sigma}$ via

$$\left.\frac{\partial\Omega}{\partial k_{M\sigma}}\right|_{\omega_{abcd}} = 0 \tag{22}$$

and continue the procedure to self-consistency. At the end of the procedure we have a functional defined purely by ω_{abcd}. The functional does not explicitly involve $k_{M\sigma}$ since these are introduced only to represent the PPLB shift. The functional can be implemented in a regular Kohn−Sham algorithm, although its performance will be limited by several factors. For example, the accuracy of the supplied E^M_{xc} and AE^M_{xc} is limited, and the functional is obtained by mapping the ab initio density quantities to the potential, while practical calculations involve self-consistent densities. In paper I, we described a corrective procedure for overcoming these errors that decreased total energy errors by an order of magnitude. This corrective procedure is very important but may be defined in many ways. In this paper we choose the following:

- The initial functional $F1$ is used to compute self-consistent total energies E^M_{tot} for systems in the training set.
- The values of the supplied atomic exchange-correlation energies E^M_{xc} are shifted by the errors in the self-consistent atomic energies E^M_{tot} to give $E^M_{\text{xc}}(2)$.
- A new functional $F2$ is computed using $E^M_{\text{xc}}(2)$ and AE^M_{xc}.
- Atomization energies are computed for each molecular system in the training set with the $F2$ functional and errors computed.
- The supplied AE^M_{xc} are shifted by the computed errors to give $AE^M_{\text{xc}}(2)$.
- A new functional $F3$ is computed using $E^M_{\text{xc}}(2)$ and $AE^M_{\text{xc}}(2)$.
- The functional is implemented, and atomic and atomization energy errors are computed.
- New estimates $E^M_{\text{xc}}(3)$ and $AE^M_{\text{xc}}(3)$ are determined from these errors, and the final functional $F4$ is computed. We find that it is not necessary to perform further iterations.

In the procedure to date we have used the energy weight $w_M = 100$. It is important to fit the energetic data well, and this value appears to give a reasonable balance between energy and potential fitting. In this work we have also reexamined the value of q in the weight $\rho^q_{M\sigma}(\mathbf{r})$ in eq 16, which was chosen to be $^2/_3$ in paper I. The exchange-correlation potential we need to fit is $v^{M\sigma}_{\text{zmp}}(\mathbf{r}) + k_{M\sigma}$, and so we have examined which value of q gives best overall agreement, paying particular attention to asymptotic regions. For the H and Ne atoms, we observe that $q = {}^1/_3$ is an improvement over $q = {}^2/_3$ in asymptotic regions, the latter resulting in a potential that becomes too positive. However, energetics are less accurate because $q = {}^1/_3$ reduces the emphasis on energetically important regions. Given that $q = {}^1/_3$ and $q = {}^2/_3$ give essentially the same potentials out to 5 bohr for both atoms, we have retained the value of $q = {}^2/_3$ in order to maintain accurate energetics.

Our calculations for this paper, together with those of paper I, have been performed self-consistently using a modified version of the CADPAC program.[16] Given the highly flexible form of our functional, it cannot be guaranteed that the final self-consistent Kohn−Sham solution will be a global minimum in the space of Kohn−Sham determinants. We can be sure only that it is a stationary point. Despite this, in virtually all of our calculations we have found the final self-consistent energy to be the lowest energy obtained during the self-consistent procedure.

This completes the outline of our procedure. The principal differences from paper I are the use of a variational procedure to compute the shifts $k_{M\sigma}$, the use of atomization energies rather than molecular total energies in the training data, and a modified final corrective procedure. In the next section we present a new functional, denoted TH2, determined according to these prescriptions.

3. TH2 Functional

The basis for the development of the TH2 functional is the TH1 functional of paper I. The terms ($^9/_6$,0,2,0) and ($^9/_6$,0,0,1) (where the notation (a,b,c,d) is used where a, b, c, and d are defined in (eq 10) have been removed as their potentials can formally diverge. Second, we have chosen to replace the terms ($^8/_6$,0,1,0) and (1,0,0,0), which can contribute a finite value to the asymptotic potential, by ($^{17}/_{12}$,0,1,0) and ($^{13}/_{12}$,0,0,0) whose potentials vanish asymptotically. All other TH1 terms have been retained.

We observe that for closed-shell systems, the term ($^{10}/_6$,0,2,0) is equivalent to a scaled Weizsacker kinetic energy functional

$$T_W = {}^1/_8\int|\nabla\rho|^2/\rho\ \mathrm{d}\mathbf{r} \tag{23}$$

For a closed-shell system, an exact solution of the Kohn−Sham equation (i.e., one that yields an exponentially decaying asymptotic density) involving this functional clearly leads to a finite system-dependent asymptotic potential (which is proportional to I, if the asymptotic density is exact). This functional would therefore appear particularly desirable. The term ($^{10}/_6$,0,0,1) is an open-shell analogue. As in paper I, we have made no effort to ensure the functional satisfies other known conditions. For example, this scaled Weizsacker term is inconsistent with exact density scaling conditions.

The functional form for TH2, together with the resulting expansion parameters from the procedure described in the previous section, are presented in Table 1. In Table 2 we present

TABLE 1: Optimized Parameters ω_{abcd} for TH2 Functional (See eq 10)

a	*b*	*c*	*d*	ω_{abcd}
$^{13}/_{12}$	0	0	0	+0.678831E+00
$^{7}/_{6}$	0	0	0	−0.175821E+01
$^{8}/_{6}$	0	0	0	+0.127676E+01
$^{9}/_{6}$	0	0	0	−0.160789E+01
$^{10}/_{6}$	0	0	0	+0.365610E+00
$^{17}/_{12}$	0	1	0	−0.181327E+00
$^{9}/_{6}$	0	1	0	+0.146973E+00
$^{10}/_{6}$	0	1	0	+0.147141E+00
$^{11}/_{6}$	0	1	0	−0.716917E−01
$^{10}/_{6}$	0	2	0	−0.407167E−01
$^{11}/_{6}$	0	2	0	+0.214625E−01
$^{12}/_{6}$	0	2	0	−0.768156E−03
$^{10}/_{6}$	0	0	1	+0.310377E−01
$^{11}/_{6}$	0	0	1	−0.720326E−01
$^{12}/_{6}$	0	0	1	+0.446562E−01
$^{7}/_{6}$	1	0	0	−0.266802E+00
$^{8}/_{6}$	1	0	0	+0.150822E+01
$^{9}/_{6}$	1	0	0	−0.194515E+01
$^{10}/_{6}$	1	0	0	+0.679078E+00

TABLE 2: Computed Values of the Shifts $k_{M\sigma}$ (in E_h) for Training Set Systems and Values for the Hardness $(I - A)/2$

	k_α	k_β	$(I - A)/2$
C	0.17	0.19	0.18
N	0.21	0.22	0.27
NH_2	0.17	0.16	0.19
CH	0.16	0.16	0.17
Li	0.12	0.54	0.09
CH_2	0.17	0.18	0.18
O	0.23	0.23	0.22
F	0.24	0.24	0.26
O_2	0.19	0.18	0.21
H	0.24		0.24
BH	0.16	0.16	
CH_4	0.18	0.18	0.37
CO	0.16	0.16	0.29
F_2	0.19	0.19	0.23
H_2	0.21	0.21	0.32
H_2O	0.20	0.20	0.35
HF	0.23	0.23	0.41
LiH	0.17	0.17	
N_2	0.16	0.16	0.33
Ne	0.28	0.28	

the computed values of $k_{M\sigma}$. As with the TH1 functional, the α shifts resemble the hardness for open-shell systems but are less than the hardness for closed-shell systems, which is consistent with theoretical requirements.

In Figure 1 we compare the self-consistent TH2 and BLYP potentials for the Ne atom. The two potentials are similar in energetically important regions but differ asymptotically. For this system the computed value of k_σ is 0.28. In Figure 2a,b we compare the BLYP and TH2 potentials with our computed near-exact potential $v_{zmp}(r) + 0.28$. Beyond approximately 2 bohr, the BLYP potential falls below this near-exact curve and rapidly approaches zero. The density is therefore too diffuse. However, the TH2 potential resembles the near-exact potential up to approximately 4 bohr, which should result in a much less diffuse density.

In Table 3 we present errors in self-consistent total energies, compared to near-exact values, for the TH2 and BLYP functionals at optimized geometries, for first-row systems both within and absent from the training set. The mean absolute errors are 6 and 18 mE_h, respectively. The corresponding value for the TH1 functional is 3 mE_h. The lower accuracy with TH2 compared to TH1 is a consequence of the new fitting procedure where the emphasis has been placed on atomization energies rather than total energies. This slight decrease in total energy accuracy is associated with a significant improvement in

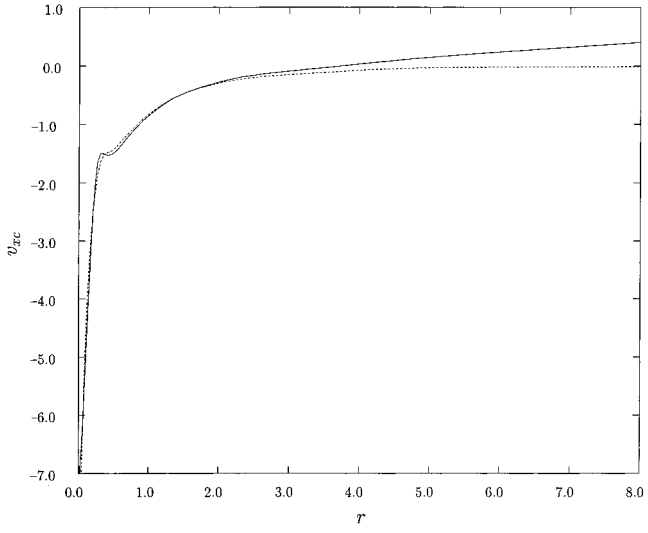

Figure 1. Comparison of self-consistent TH2 (solid curve) and BLYP (dotted curve) potentials for the Ne atom (in au), plotted as a function of radial distance.

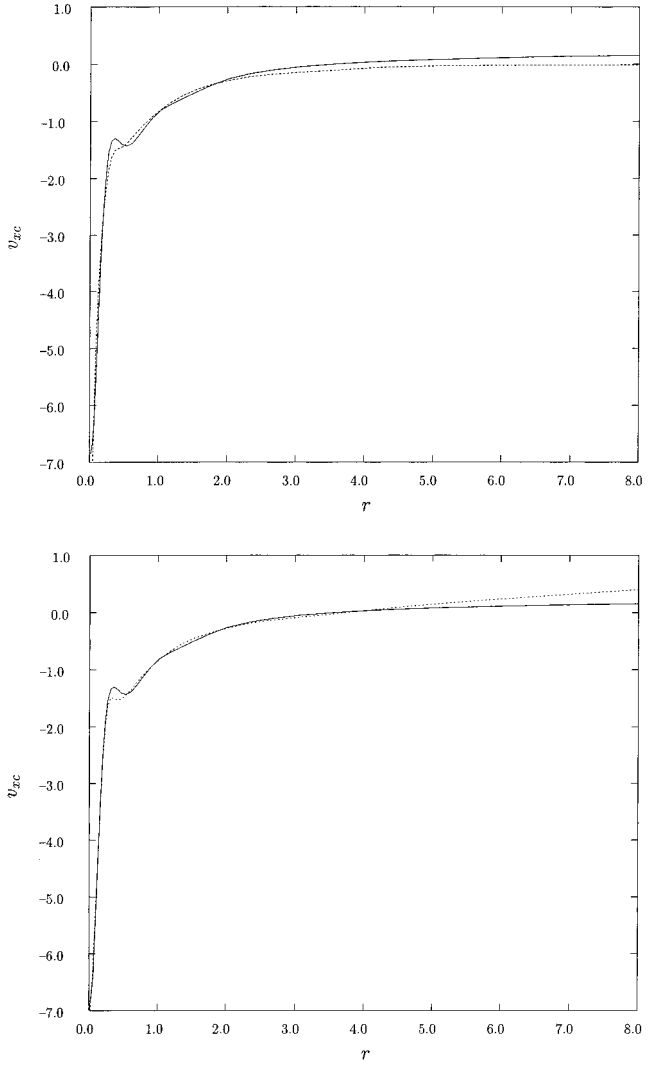

Figure 2. Near-exact continuum potential $v_{zmp}(r) + 0.28$ (solid curve) for the Ne atom (in au), plotted as a function of radial distance, compared with self-consistent (a, top) BLYP and (b, bottom) TH2 potentials (dotted curves).

TABLE 3: Near-Exact Total Energies $E_{tot,0}$ and Errors in Self-Consistent TH2 and BLYP Total Energies (All Quantities in E_h) for Systems Both Within and Absent from the Training Set

	$E_{tot,0}$	$E_{tot}^{TH2} - E_{tot,0}$	$E_{tot}^{BLYP} - E_{tot,0}$
H_2	−1.174	−0.003	+0.005
H_2O	−76.437	+0.007	−0.011
CO	−113.325	+0.001	−0.023
F_2	−199.529	−0.006	−0.071
N_2	−109.543	+0.003	−0.017
HF	−100.458	+0.004	−0.023
LiH	−8.070	−0.005	+0.002
CH_4	−40.513	+0.005	+0.011
H	−0.500	+0.001	+0.005
Li	−7.478	−0.003	−0.003
C	−37.845	+0.002	−0.002
N	−54.589	−0.001	−0.001
O	−75.067	−0.004	−0.018
F	−99.734	+0.001	−0.027
Ne	−128.939	+0.000	−0.019
CH	−38.479	−0.001	−0.002
CH_2	−39.148	+0.011	+0.003
O_2	−150.326	−0.017	−0.058
NH_2	−55.879	+0.004	−0.006
C_2H_2	−77.376	+0.007	+0.003
C_2H_4	−78.586	+0.009	+0.009
C_2H_6	−79.823	+0.015	+0.021
CO_2	−188.599	−0.003	−0.053
H_2CO	−114.507	+0.002	−0.020
H_2O_2	−151.562	+0.004	−0.041
HCN	−93.431	+0.001	−0.012
Li_2	−14.995	+0.006	+0.001
N_2H_4	−111.876	+0.014	−0.003
NH_3	−56.563	+0.007	+0.002
O_3	−225.434	−0.017	−0.089
CH_3OH	−115.728	+0.012	−0.007
Δ		0.006	0.018

TABLE 4: Experimental Total Atomization Energies ($\sum D_0$) and Errors in Self-Consistent BLYP, TH1, and TH2 Atomization Energies ($\sum D_0^{calc} - \sum D_0$) (All Quantities in kcal/mol) for Systems Both Within and Absent from the Training Set

	BLYP	TH1	TH2	expt
H_2	+2.2	−0.3	+2.4	103.5
H_2O	+1.7	+1.0	−5.5	219.3
CO	+1.7	+3.5	−1.4	256.2
F_2	+11.1	+20.0	+5.7	36.9
N_2	+9.5	−8.7	−3.1	225.1
HF	+0.5	+5.7	−1.1	135.2
LiH	−0.4	−1.4	+1.3	56.0
CH_4	+2.8	−4.5	+0.4	392.5
CH	+2.6	−1.8	+2.8	79.9
CH_2	+2.6	−3.5	−4.2	179.6
O_2	+14.4	+18.9	+6.2	118.0
NH_2	+9.3	−6.8	−2.0	170.0
C_2H_2	+1.0	−6.0	−0.7	388.9
C_2H_4	+2.7	−6.5	−0.4	531.9
C_2H_6	+0.9	−10.3	−3.5	666.3
CO_2	+9.4	+14.0	−1.4	381.9
H_2CO	+5.9	+3.8	−0.7	357.2
H_2O_2	+9.2	+8.3	−5.9	252.3
HCN	+8.4	−5.0	+0.7	301.8
Li_2	−4.3	−9.3	−7.6	24.0
N_2H_4	+12.7	−14.0	−7.6	405.4
NH_3	+6.8	−7.8	−3.4	276.7
O_3	+22.6	+28.4	+4.0	142.2
CH_3OH	+3.2	−2.4	−6.4	480.8
Δ	6.1	8.0	3.3	

computed atomization energies, as shown in Table 4 (the zero-point contributions to the atomization energies are taken from ref 15). The errors from TH1 are unacceptably large, and it was this observation that led us to introduce atomization energies into the fitting procedure. The TH2 functional has a mean absolute error of 3.3 kcal/mol, compared to 8.0 and 6.1 kcal/mol with TH1 and BLYP. In particular, we note that errors for the difficult systems F_2, O_2, CO_2, N_2H_4, and O_3 are substantially improved with TH2.

Despite this success, a word of caution is necessary. The TH2 functional has been developed by training on a small set of first-row systems. Our results demonstrate that it can be usefully applied to other first-row molecules, although there is no reason to expect the functional to be as successful for systems that differ significantly to those in the training set. A preliminary study on second-row molecules indicates that while TH2 structures are at least comparable to those from BLYP, atomization energies are considerably less accurate. However, the study also suggests that the introduction of second-row systems into the training set can significantly reduce these errors.[17] Like the TH1 functional, TH2 should therefore be interpreted as a first-row functional.

4. Hydrogen Abstraction Reactions

In a recent study, Skokov and Wheeler[18] examined the six hydrogen abstraction reactions

$$H_2 + H \rightarrow H + H_2 \quad \text{(I)}$$

$$CH_4 + CH_3 \rightarrow CH_3 + CH_4 \quad \text{(II)}$$

$$H_2 + CH_3 \rightarrow H + CH_4 \quad \text{(III)}$$

$$H_2 + NH_2 \rightarrow H + NH_3 \quad \text{(IV)}$$

$$H_2 + OH \rightarrow H + H_2O \quad \text{(V)}$$

$$CH_4 + OH \rightarrow CH_3 + H_2O \quad \text{(VI)}$$

and concluded that the hybrid functionals B3LYP and B3P86[19−21] gave significantly improved reaction barriers compared to the continuum density functionals BLYP and BP86. Such hydrogen abstraction reactions are a keen test of DFT because of the creation of an apparent "extra bond" at the transition state. The failure of conventional functionals to describe reaction I was previously highlighted by Johnson et al.,[22] and a detailed study of reaction V was performed by Baker et al.[23] We have performed calculations using the BLYP, B3LYP, and TH2 functionals on these six reactions, using the TZ2P basis set. Tables 5 and 6 present optimized transition-state structures (each confirmed as having a single imaginary harmonic vibrational frequency) and classical reaction barriers for the six reactions. These are compared with results from high-level ab initio calculations.

Reaction I, the simplest possible hydrogen abstraction reaction, is troublesome for existing functionals. BLYP overestimates the bond length and significantly underestimates the reaction barrier; the bond length is improved with the B3LYP functional, although the barrier is still too low by more than a factor of 2. In contrast, the TH2 functional yields a bond length comparable to B3LYP, with a much improved reaction barrier.

BLYP provides a much improved description for reactions II and III, although the barriers are still too low. Once again, the barrier increases with the introduction of exact exchange in B3LYP. For these reactions, the TH2 prediction is comparable to BLYP.

TABLE 5: Transition-State Structures (in Å and deg) Computed Using BLYP, B3LYP, and TH2 Functionals, Compared to ab Initio Values

quantity	BLYP	B3LYP	TH2	ab initio
		H− H′−H		
R(H−H′)	0.936	0.930	0.931	0.930[a]
		CH_3−H′−CH_3		
R(C−H′)	1.359	1.348	1.362	1.36[b]
		CH_3−H′−H″		
R(C−H′)	1.410	1.394	1.401	1.393[c]
R(H′−H″)	0.905	0.903	0.909	0.897[c]
θ(H−C−H′)	103.3	103.5	103.5	103.7[c]
		NH_2−H′−H″		
R(N−H′)	1.353	1.314	1.311	1.307[c]
R(H′−H″)	0.881	0.891	0.903	0.890[c]
θ(N−H′−H″)	162.1	161.4	162.8	158.7[c]
		HO−H′−H″		
R(O−H′)		1.406	1.525	1.329[c]
R(H′−H″)		0.808	0.787	0.829[c]
θ(O−H′−H″)		163.4	164.1	162.8[c]
		CH_3−H′−OH		
R(C−H′)		1.222	1.227	1.181[d]
R(O−H′)		1.313	1.342	1.330[d]
θ(C−H′−O)		173.4	174.3	172.1[d]

[a] Reference 24. [b] Reference 25. [c] Reference 26. [d] Reference 27.

TABLE 6: Classical Reaction Barriers (in kcal/mol) Computed Using BLYP, B3LYP, and TH2 Functionals, Compared to ab Initio Values

reaction	BLYP	B3LYP	TH2	ab initio
I	2.76	4.01	7.88	9.61[a]
II	13.64	15.92	13.35	17.5[b]
III	8.14	9.78	8.95	11.81[c]
IV	3.51	6.33	5.86	9.51[c]
V		1.23	0.89	5.62[c]
VI		2.58	0.48	6.62[d]

[a] Reference 24. [b] Reference 25. [c] Reference 26. [d] Reference 27.

Reaction IV is a difficult case for BLYP. The barrier is significantly too low, and the transition state occurs much too early in the reaction profile—i.e., at a large $NH_2\cdots H_2$ distance. The B3LYP and TH2 structures and reaction barriers are comparable and are a significant improvement over BLYP.

Reaction V is particularly interesting. Baker et al.[23] examined the system for a range of fixed $H_2\cdots OH$ distances. With the BLYP functional, they observed a transition state whose energy was below the energy of the reactants. (The same observation was made in ref 18.) With a very extensive basis set, Baker et al. did not observe this feature in their range of $H_2\cdots OH$ distances, and so the reaction profile became purely attractive. In contrast, their B3LYP results exhibited a well-defined positive reaction barrier. Like Skokov and Wheeler, this study led Baker et al. to stress the importance of exact exchange in describing this abstraction reaction. Our BLYP results for this reaction are consistent with these earlier studies. In our attempt to locate a transition state, the $H_2\cdots OH$ distance slowly increases to 2.8 Å, at which stage the gradient falls below the required tolerance to define a transition state. The energy of the resulting structure lies below that of the reactants. However, given that the surface is very flat and that Baker et al. demonstrated that the position of this feature is strongly basis set dependent, we do not assign any physical significance to the feature and simply conclude that the BLYP description is incorrect, as it does not predict any physical barrier. Our B3LYP calculations do predict a positive reaction barrier, although it occurs earlier in the reaction profile than the ab initio result. The TH2 functional also predicts

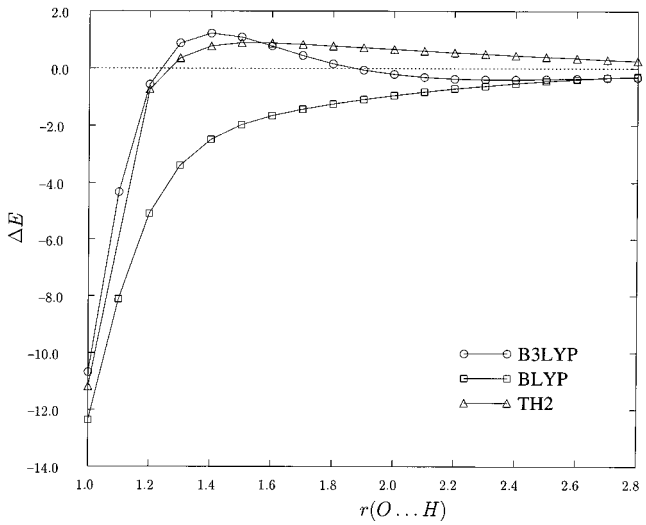

Figure 3. Reaction profiles for $H_2 + OH \rightarrow H + H_2O$ with the B3LYP, BLYP, and TH2 functionals. The energy (in kcal/mol) is relative to the reactants.

a positive barrier, even earlier in the reaction profile than for B3LYP. In Figure 3 we summarize these results by plotting reaction profiles for this reaction using the three functionals. Following Baker et al. we optimize structures for a variety of fixed $H_2\cdots OH$ separations; energies are relative to the reactants. Like BLYP, the B3LYP profile is attractive at large separation, although it becomes repulsive as the reactants approach one another. The TH2 profile is repulsive right up to the transition state.

The results for reaction VI are analogous to those of reaction V. BLYP predicts an attractive energy profile with no physical barrier. Both the TH2 and B3LYP functionals yield physical transition states, whose geometries agree well with the best ab initio values. The barrier with TH2 is significantly lower than the B3LYP value.

Next, consider experimental reaction barriers rather than ab initio ones. To compare with these quantities, several corrections must be made to the computed classical barriers in Table 6. First, basis set superposition errors (BSSE) must be accounted for. Our calculations demonstrate that the BSSE is largest for the BLYP functional and smallest for TH2. BSSE corrections increase the barrier by between 0.13 and 0.36 kcal/mol for the TH2 functional. Following Kraka et al.[26] we also include vibrational corrections at 300 K as defined in ref 28 which can raise the barriers by up to 0.7 kcal/mol (neglecting the lowest mode in reactions II and VI), and Wigner tunneling[29] corrections at 300 K:

$$\Delta E = -kT\frac{u^2}{12(1+u^2/24)} \qquad u = h\nu/\mathrm{kT} \qquad (24)$$

where ν is the magnitude of the imaginary harmonic frequency. This term can lower the barriers by up to 0.9 kcal/mol. The largest correction to the classical barrier arises due to zero-point vibrations, which vary between −1.1 and +2.1 kcal/mol. We have not included any other temperature effects due to changes in the number of translational and rotational degrees of freedom, as we are uncertain of their theoretical justification for transition-state reactions. In Table 7, we compare these corrected barriers with experimental values. (It is clear from the experimental papers that there is some uncertainty in the experimental barriers, typically 0.5 kcal/mol, for several of these reactions.) Both the B3LYP and TH2 functionals have a mean absolute error of less

TABLE 7: Classical Reaction Barriers (in kcal/mol), Corrected for BSSE, Zero-Point Vibrations, Thermal Vibrational Effects, and Wigner Tunneling, Computed Using BLYP, B3LYP, and TH2 Functionals, Compared to Experimental Values

reaction	BLYP	B3LYP	TH2	expt
I	2.31	3.19	6.97	9.7[a]
II	13.10	15.27	12.70	14.3[b]
III	9.74	11.14	10.42	10.7[c]
IV	5.91	8.40	7.69	8.5[d]
V		2.39	2.50	4.0[e]
VI		1.61	−0.12	3.7[f]

[a] Reference 30. [b] Reference 31. [c] Reference 32. [d] Reference 33. [e] Reference 34. [f] Reference 35.

TABLE 8: Reaction Energies (in kcal/mol) Computed Using BLYP, B3LYP, and TH2 Functionals, Compared to ab Initio Values

reaction	BLYP	B3LYP	TH2	ab initio
III	+0.42	+0.30	−2.60	−4.01[a]
IV	−1.69	−1.60	−2.71	−6.39[a]
V	−12.00	−10.80	−11.70	−16.65[a]
VI	−12.41	−11.11	−9.10	−12.10[b]

[a] Reference 26. [b] Reference 27.

than 2 kcal/mol for these six reactions, which is a significant improvement over BLYP.

It is clear from the above results that an improved description of hydrogen abstraction reaction barriers can be obtained without the need to introduce a fraction of exact orbital exchange. In addition, it is sometimes claimed that a reason for the failure of conventional continuum density functionals to yield accurate barriers is the issue of self-interaction. We have not specifically addressed this issue, although the shifted ZMP potentials in the fitting procedure are, in principle, the functional derivatives of a functional that correctly accounts for self-interaction. We believe a principal reason for the success of TH2 is that it was developed using a knowledge of exchange-correlation potentials and so should yield improved asymptotic densities, which may be important for an accurate description of the transition from reactants to products. Finally, we mention total reaction energies. In Table 8 we compare BLYP, B3LYP, and TH2 reaction energies for reactions III−VI with ab initio results.[26,27] The TH2 functional correctly predicts all four reactions to be exoergic, and the reasonable accuracy suggests that the functional can also provide a reasonable description of the barrier heights for the reverse endoergic reactions.

5. Conclusion

In this paper, we have presented a new first-row GGA exchange-correlation functional, denoted TH2, obtained using a modified version of the method described in paper I. By introducing atomization energies into the fitting procedure we have significantly reduced the atomization energy errors of the TH1 functional, with only a slight decrease in absolute energy accuracy. We have used the TH2 functional to study six simple first-row hydrogen abstraction reactions. For the reactions where the BLYP description is reasonable, the TH2 results are comparable to BLYP. In the reactions where the BLYP reaction barrier is poor, the TH2 functional is a significant improvement. For the two cases where BLYP completely fails to predict a reaction barrier, the TH2 functional, like B3LYP, does predict a positive barrier. The results demonstrate that improved hydrogen abstraction reaction barriers can be obtained without introducing a fraction of exact orbital exchange into the functional.

Acknowledgment. We are grateful to Professor R. A. Wheeler for providing a preprint of ref 18 and to Dr. S. Skokov for clarifying the definition of the tunneling correction to the barrier.

References and Notes

(1) Tozer, D. J.; Handy, N. C. *J. Chem. Phys.* **1998**, *108*, 2545.
(2) Sharp, R. T.; Horton, G. K. *Phys. Rev.* **1953**, *90*, 317. Talman, J. D.; Shadwick, W. F. *Phys. Rev. A* **1976**, *14*, 36. Grabo, T.; Gross, E. K. U. *Chem. Phys. Lett.* **1995**, *240*, 141. Engel, E.; Vosko, S. H. *Phys. Rev. A* 47 2800 1993.
(3) Handy, N. C.; Marron, M. T.; Silverstone, H. J. *Phys. Rev.* **1969**, *180*, 45.
(4) Chan, G. K.-L; Tozer, D. J.; Handy, N. C. *J. Chem. Phys.* **1997**, *107*, 1536.
(5) Dirac, P. A. M. *Proc. Cam. Philos. Soc.* **1930**, *26*, 376. Vosko, S. J.; Wilk, L.; Nusair, M. *Can. J. Phys.* **1980**, *58*, 1200.
(6) Tozer, D. J.; Handy, N. C.; Green, W. H. *Chem. Phys. Lett.* **1997**, *273*, 183.
(7) Perdew, J. P.; Parr, R. G.; Levy, M.; Balduz, Jr., J. L. *Phys. Rev. Lett.* **1982**, *49*, 1691.
(8) Perdew, J. P.; Burke, K. *Int. J. Quantum. Chem.* **1996**, *57*, 309.
(9) Becke, A. D. *Phys. Rev. A* **1988**, *38*, 3098. Lee, C.; Yang, W.; Parr, R. G. *Phys. Rev. B* **1988**, *37*, 785.
(10) Levy, M.; Perdew, J. P.; Sahni, V. *Phys. Rev. A* **1984**, *30*, 2745.
(11) Kobayashi, R.; Amos, R. D.; Handy, N. C. *J. Chem. Phys.* **1994**, *100*, 1375.
(12) Huzinaga, S. *J. Chem. Phys.* **1965**, *42*, 1293.
(13) Dunning, T. H. *J. Chem. Phys.* **1971**, *55*, 716.
(14) Zhao, Q.; Morrison, R. C.; Parr, R. G. *Phys. Rev. A* **1994**, *50*, 2138.
(15) Davidson, E. R.; Hagstrom, S. A.; Chakravorty, S. J.; Meiser Umor, V.; Froese Fischer, C. *Phys. Rev. A* **1991**, *44*, 7071. Curtiss, L. A.; Raghavachari, K.; Trucks, G. W.; Pople, J. A. *J. Chem. Phys.* **1991**, *94*, 7221. Pople, J. A.; Head-Gordon, M.; Fox, D. J.; Raghavachari, K.; Curtiss, L. A. *J. Chem. Phys.* **1989**, *90*, 5622.
(16) Amos, R. D.; Alberts, I. L.; Andrews, J. S.; Colwell, S. M.; Handy, N. C.; Jayatilaka, D.; Knowles, P. J.; Kobayashi, R.; Laming, G. J.; Lee, A. M.; Maslen, P. E.; Murray, C. W.; Palmieri, P.; Rice, J. E.; Simandiras, E. D.; Stone, A. J.; Su, M.-D.; Tozer, D. J. CADPAC6.0, The Cambridge Analytic Derivatives Package, Cambridge, UK, 1995.
(17) Handy, N. C.; Tozer, D. J. *Mol. Phys.*, in press.
(18) Skokov, S.; Wheeler, R. A. *Chem. Phys. Lett.* **1997**, *271*, 251.
(19) Becke, A. D. *J. Chem. Phys.* **1993**, *98*, 5648.
(20) Stephens, P. J.; Devlin, F. J.; Chabalowski, C. F.; Frisch, M. J. *J. Phys. Chem.* **1994**, *98*, 11623.
(21) Perdew, J. P.; Wang, Y. *Phys. Rev. B* **1986**, *33*, 8822.
(22) Johnson, B. G.; Gonzales, C. A.; Gill, P. M. W.; Pople, J. A. *Chem. Phys. Lett.* **1994**, *221*, 100.
(23) Baker, J.; Andzelm, J.; Muir, M.; Taylor, P. R. *Chem. Phys. Lett.* **1995**, *237*, 53.
(24) Diedrich, D. L.; Anderson, J. B. *Science* **1992**, *258*, 786.
(25) Musgrave, C.; Perry, J. K.; Merkle, R. C.; Goddard, III, W. A. *Nanotechnology* **1991**, *2*, 187.
(26) Kraka, E.; Gauss, J.; Cremer, D. *J. Chem. Phys.* **1993**, *99*, 5306.
(27) Dobbs, K. D.; Dixon, D. A.; Komornicki, A. *J. Chem. Phys.* **1993**, *98*, 8852.
(28) Del Bene, J. E.; Mettee, H. D.; Frisch, M. J.; Luke, B. T.; Pople, J. A. *J. Phys. Chem.* **1983**, *87*, 3279.
(29) Wigner, E. *Z. Physik Chem. B.* **1932**, *19*, 203.
(30) Schulz, W. R.; LeRoy, D. J. *J. Chem. Phys.* **1965**, *42*, 3869.
(31) Tedder, J. M. *Angew. Chem., Int. Ed. Engl.* **1982**, *21*, 401.
(32) Schatz, G. C. Wagner, A. F.; Dunning, T. H. *J. Phys. Chem.* **1984**, *88*, 221.
(33) Demissy, M.; Lesclaux, R. *J. Am. Chem. Soc.* **1980**, *102*, 2897.
(34) Tully, F. P.; Ravishankara, A. R. *J. Phys. Chem.* **1980**, *84*, 3126.
(35) Baulch, D. L.; Bowers, M.; Malcolm, D. G.; Tuckerman, R. T. *J. Phys. Chem. Ref. Data* **1986**, *15*, 465.